

# MULTISCALE TRANSFORMS FOR REGION-BASED TEXTURE SEGMENTATION

Jalal M. Fadili<sup>1</sup>, François Lecellier<sup>2</sup> and Stéphanie Jehan-Besson<sup>3</sup>

<sup>1</sup> GREYC CNRS-ENSICAEN-Université de Caen, Caen France

<sup>2</sup> XLIM CNRS-Université de Poitiers, Poitiers France

<sup>3</sup> LIMOS CNRS, Clermond-Ferrand France

Emails: Jalal.Fadili@greyc.ensicaen.fr, francois.lecellier@univ-poitiers.fr, jehan@isima.fr

## ABSTRACT

In this paper we propose a rigorous and elegant framework for texture image segmentation relying on region-based active contours (RBAC), shape derivative tools and multiscale geometrical texture representations. After transforming the texture in a dictionary of appropriate waveforms (atoms), the obtained transform coefficients are intended to efficiently capture the essential spectral and geometrical contents of the texture, and to allow to discriminate it from other textures. Hence, to measure the dissimilarity between two different textures, we use a divergence between the non-parametric kernel density estimates of the probability density functions (PDFs) of their respective transform coefficients. The divergence measure is then either minimized (supervised segmentation) or maximized (unsupervised) after appropriately incorporating it within an RBAC variational functional. The functional is then optimized by taking benefit from shape derivative tools to derive the evolution equation of the active contour. Our framework is applied to both supervised (with exemplar reference textures), and unsupervised texture segmentation. A series of experiments on synthetic and real images are reported to illustrate the versatility and applicability of our approach.

## 1. INTRODUCTION

Texture segmentation remains a difficult and challenging task, and an intense research field. Indeed, the main bottleneck to segment a texture image is to find an appropriate set of generic computable descriptors to characterize a given texture and discriminate distinct textures between them. Representing and characterizing textures remains an important open problem, mainly because there is no consensus on how to define a texture model, despite several attempts including random models in spatial or transform domains, low-dimensional manifold models, or sparsity-oriented models; see [10] for an review. There is also number of papers devoted to the segmentation of textured images; a comprehensive overview can be found e.g. in [7]. Some of them attacked the problem of segmenting or classifying textures using the wavelet machinery as texture descriptors [12, 5, 2, 3]. In this paper, we tackle the texture segmentation

This work was accomplished when the second and third authors were hosted in the first institution.

problem under the umbrella of transform domain models such as, but not limited to, wavelets, and variational region-based active contours (RBAC). More precisely, we propose a general texture segmentation framework that discriminates textures by measuring a divergence between the non-parametric density estimates of the PDFs of their respective transform coefficients. The framework is adapted to both supervised and unsupervised segmentation of textured images. In the supervised case (Section 3.1.1), we consider the minimization of the divergence between the coefficients PDF of a reference exemplar texture, and that of the texture to segment. In the unsupervised case (Section 3.1.2), we maximize this divergence between the coefficients PDFs.

**Region-based active contours and shape derivatives** In variational image segmentation, the general energy functional to be optimized is composed of region and contour terms. For the sake of simplicity, we will focus in the sequel on the 2D case. Let  $\Omega_I$ , an open bounded subset of  $\mathbb{R}^2$ , be the domain of the image. Image segmentation can then be cast as obtaining a disjoint minimal partition of  $\Omega_I$  in  $K \geq 2$  regions

$$\min_{\{\Omega_k\}_{k=1}^K \mid \bigcup_{k=1}^K \Omega_k \cup \partial\Omega = \Omega_I} F(\Omega_1, \dots, \Omega_K, \partial\Omega) = \sum_{k=1}^K \int_{\Omega_k} F_k(\mathbf{x}; \Omega_k) d\mathbf{x} + \int_{\partial\Omega} F_b(\mathbf{x}) ds(\mathbf{x}), \quad (1)$$

where  $F_k$  is the region descriptor attached to the open bounded and regular domain/region  $\Omega_k$ ,  $\partial\Omega$  is the boundary of the regions, and  $s(\mathbf{x})$  is the curvilinear abscissa. Each descriptor  $F_k$  can be thought of as a homogeneity criterion, where homogeneity is to be understood in a broad sense. The contour integral term corresponds to a local information, and can be used as a regularization on  $\partial\Omega$ . Typically, this term can be the length of the contour (as a curve) in 2D in which case  $F_b(\mathbf{x}) = \lambda$ , a positive constant that plays the role of a regularization parameter.

Once the optimization problem has been formulated, it remains now to solve it with respect to the domains  $\{\Omega_k\}_{k=1, \dots, K}$ , by deriving a geometrical evolution PDE that would drive the contour to a stationary point of the minimized energy functional, which may happen to be a local minimum of interest. However, the set of domains in  $\mathbb{R}^d$  does not have the structure of a vector space, and classical descent algorithms do not qual-

ify straightforwardly for this problem. Throughout this work, to exhibit such a PDE, we will focus on shape derivative tools.

To cut a long story short, shape derivative tools consist in considering that the domain evolves in a velocity field  $\mathbf{V}$ , and the derivative of a domain functional  $F_r(\Omega) := \int_{\Omega} F(\mathbf{x}; \Omega) d\mathbf{x}$  is computed in the direction  $\mathbf{V}$ . This is summarized in the following result.

**Theorem 1 ([4, 6])** *The Eulerian derivative of the domain functional  $F_r(\Omega)$  in the direction  $\mathbf{V}$  is given by*

$$\langle F_r'(\Omega), \mathbf{V} \rangle = \int_{\Omega} F'(\mathbf{x}; \Omega, \mathbf{V}) d\mathbf{x} - \int_{\partial\Omega} F(\mathbf{x}; \Omega) \langle \mathbf{V}, \mathbf{N} \rangle d\mathbf{a}(\mathbf{x}),$$

where  $\mathbf{N}$  is the inward unitary normal to  $\partial\Omega$ ,  $d\mathbf{a}(\mathbf{x})$  the area element, and  $F'(\mathbf{x}; \Omega, \mathbf{V})$  is the domain derivative of  $F(\mathbf{x}; \Omega)$  in the direction  $\mathbf{V}$ :

$$F'(\mathbf{x}; \Omega, \mathbf{V}) = \lim_{\tau \rightarrow 0} \frac{F(\mathbf{x}; \Omega(\tau)) - F(\mathbf{x}; \Omega)}{\tau}.$$

With this derivative at hand, the evolution PDE of the active contour  $\Gamma(\tau)$  is given by

$$\frac{\partial \Gamma}{\partial \tau} = \text{speed}(\mathbf{x}; \Omega) \cdot \mathbf{N}, \quad \Gamma(\tau = 0) = \Gamma_0, \quad (2)$$

if one is able to re-express the Eulerian derivative of  $F_r(\Omega)$  as

$$\langle F_r'(\Omega), \mathbf{V} \rangle = - \int_{\partial\Omega} \text{speed}(\mathbf{x}; \Omega) \langle \mathbf{V}, \mathbf{N} \rangle d\mathbf{a}(\mathbf{x}). \quad (3)$$

## 2. TEXTURE DESCRIPTORS

Sparsity in fixed or learned dictionaries has been successfully used for texture synthesis and also for texture segmentation and classification. For these tasks, most fixed dictionaries can be viewed as a cascade of filter banks. These filter banks are built in order to discriminate between the textures depending on their frequency response. However, many of these methods are designed to a particular choice of the transform. On the other hand, this choice will obviously not be adapted for a variety of textures. For instance, it has been known for some time now that some transforms can entail reasonably sparse expansions of certain textures; e.g. locally oscillatory textures in bases such as local discrete cosines [11], brushlets [9], Gabor [8], wave-atoms [13]. Gabor and dyadic traditional wavelets are widely used in the image processing community for texture analysis. Their use may be motivated by physiological evidence where simple cells of the primary visual cortex exhibit Gabor-like responses. But little is known on the decay, hence the approximation behavior, of wavelet coefficients of textures in general. In fact, sparsely representing realistic models of textures remains an open problem.

Our goal here is to segment textures in images without confining ourselves to a specific representation to characterize them, nor necessarily relying on the sparsity of the transform coefficients (see Section 3.1.1). Thus, our framework is flexible enough to handle virtually any transform which is able

to discriminate the targeted textures. For good success of the segmentation, such a transform should satisfy three major requirements: (i) to be multiscale; (ii) translation invariant; and (iii) to enjoy directional selectivity. Note that multiscale and translation invariance are reminiscent of the axioms of random generative models popular in statistical modeling of natural images.

We denote by  $\alpha_{\gamma} = \langle f, \varphi_{\gamma} \rangle$  the coefficients of a texture  $f$  in a dictionary of atoms  $\{\varphi_{\gamma}\}$ , where  $\gamma = (j, \theta_j, \mathbf{x})$ ,  $j \geq 0$  is the scale,  $\theta_j \in [0, 2\pi[$  the subband/orientation parameter at scale  $j$ , and  $\mathbf{x} = (x_1, x_2)$  the position. For instance, for the TI-wavelet transform,  $\gamma$  is:  $j \in \{0, \dots, J-1\}$  and  $\theta_j \in \{0, \pi/4, \pi/2\}$  for all  $j$ . For wave-atoms:  $j \in \{0, \dots, \lceil \frac{J-1}{2} \rceil + 1\}$  and  $\theta_j$  is implicit in  $j$  such that  $\nu_{j, \mathbf{m}} = \pm \pi \mathbf{m} 2^j \sim 2^{2j}$ , where  $\nu_{j, \mathbf{m}}$  is the central frequency of the wave-atom,  $\mathbf{m} = (m_1, m_2)$ ,  $(m_1, m_2)$  is a pair of integers such that  $\max_{i=1,2} m_i \sim 2^j$ . This relation be-

tween the central frequency and the support size of the wave-atom is behind a parabolic scaling law which entails that wave-atoms provide optimally sparse representation of locally warped oscillatory patterns [13].

## 3. PDF-BASED TEXTURE SEGMENTATION

Hitherto, we have advocated the use of transform coefficients as discriminative descriptors to reveal the differences between different textures depending on their spectral and geometrical contents. Once the transform has been identified, it remains now to compare these texture descriptors (coefficients), and we here propose to use a divergence between their respective PDFs. Under stationarity hypothesis in each subband  $(j, \theta_j)$ , the proposed domain functional to be optimized reads:

$$F_{j, \theta_j}(\Omega) = \int_{\mathcal{X}} \mathcal{D} \left( \text{pdf}_{j, \theta_j}^1(\alpha; \Omega), \text{pdf}_{j, \theta_j}^2(\alpha; \Omega) \right) d\alpha, \quad (4)$$

where  $\mathcal{D} : \mathbb{R}^+ \times \mathbb{R}^+ \rightarrow \mathbb{R}^+$  is some metric comparing two PDFs  $\text{pdf}_{j, \theta_j}^1$  and  $\text{pdf}_{j, \theta_j}^2$ . Typical choices of  $\mathcal{D}$  including the Hellinger distance, the  $\chi^2$ -score, or the Kullback-Leibler divergence (KLD) or its symmetrized version (which is in fact a distance), etc. Summing (4) over scales and subbands, segmenting a texture amounts to optimizing the following domain functional:

$$F(\Omega) = \sum_{j, \theta_j} F_{j, \theta_j}(\Omega). \quad (5)$$

### 3.1. Supervised segmentation

Supervised segmentation means that an exemplar texture is available to serve as a reference and for which the coefficients PDF at all subbands are known a priori. Given a new candidate image containing a similar texture, the goal is to segment it. In the notation of (4), one of the PDFs (e.g.  $\text{pdf}_{j, \theta_j}^2$ ) would be that of the exemplar  $\text{pdf}_{j, \theta_j}^{\text{ref}}$ , which obviously does not depend on  $\Omega$ .

#### 3.1.1. Parametric approach

The path undertaken here strongly relies on the sparsity of the texture representation coefficients at all scales and subbands in

the domain of the chosen transform. If such a hypothesis holds true, then a good candidate sparsity-promoting prior PDF would be the generalized Gaussian distribution (GGD) family. With the symmetrized KLD, (5) becomes:

$$F(\Omega) = \sum_{j,\theta_j} \left( \frac{\sigma_{j,\theta_j}^{\text{ref}}}{\sigma_{j,\theta_j}(\Omega)} \right)^{p_{j,\theta_j}(\Omega)} \frac{\Gamma\left(\frac{1+p_{j,\theta_j}(\Omega)}{p_{j,\theta_j}^{\text{ref}}}\right)}{\Gamma\left(\frac{1}{p_{j,\theta_j}^{\text{ref}}}\right)} + \left( \frac{\sigma_{j,\theta_j}(\Omega)}{\sigma_{j,\theta_j}^{\text{ref}}}\right)^{p_{j,\theta_j}^{\text{ref}}} \frac{\Gamma\left(\frac{1+p_{j,\theta_j}^{\text{ref}}}{p_{j,\theta_j}(\Omega)}\right)}{\Gamma\left(\frac{1}{p_{j,\theta_j}(\Omega)}\right)} - \frac{1}{p_{j,\theta_j}(\Omega)} - \frac{1}{p_{j,\theta_j}^{\text{ref}}}, \quad (6)$$

where  $p_{j,\theta_j}(\Omega)$  and  $\sigma_{j,\theta_j}(\Omega)$  are the shape and scale parameters of GGD distribution at each scale and subband,  $\Gamma(z)$  is the Gamma function. These parameters are estimated in each region during the contour evolution, hence their dependence on the domain  $\Omega$ . Using a moment estimators yields:

$$p_{j,\theta_j}^{\text{MO}}(\Omega) = h^{-1} \left( \frac{\left(M_{j,\theta_j}^{(1)}(\Omega)\right)^2}{M_{j,\theta_j}^{(2)}(\Omega)} \right), \quad (7)$$

$$\sigma_{j,\theta_j}^{\text{MO}}(\Omega) = \frac{M_{j,\theta_j}^{(1)}(\Omega) \Gamma\left(\frac{1}{p_{j,\theta_j}^{\text{MO}}(\Omega)}\right)}{\Gamma\left(\frac{2}{p_{j,\theta_j}^{\text{MO}}(\Omega)}\right)}, \quad (8)$$

where  $h(p) = \frac{\Gamma^2(\frac{2}{p})}{\Gamma(\frac{1}{p})\Gamma(\frac{3}{p})}$ , and  $M_{j,\theta_j}^{(i)}(\Omega) := \frac{1}{|\Omega|} \int_{\Omega} |\alpha_{j,\theta_j,\mathbf{x}}|^i d\mathbf{x}$  is the absolute empirical moment of order  $i$ . Beyond existence and uniqueness issues of these estimators<sup>1</sup>, their implicit form makes the derivation of the evolution PDE through the Eulerian derivative of  $F(\Omega)$  (see Theorem 1) cumbersome. Furthermore, such an approach is strongly sensitive to the sparsity/compressibility assumption which may be violated for some textures. To mitigate these limitations, we now move to the much more versatile non-parametric approach.

### 3.1.2. Non-parametric approach

**Kernel density estimators** Given a collection of observed coefficient samples, supposed to be independent and identically distributed, this approach will first estimate the underlying PDF using the well-known kernel density estimator. Let  $K_{\varsigma}$  a positive kernel of unit mass and bandwidth  $\varsigma$ . The kernel density estimator of  $\text{pdf}_{j,\theta_j}^1$  in (4) is defined as

$$\text{pdf}_{j,\theta_j}^1(\alpha; \Omega) = \frac{1}{|\Omega|} \int_{\Omega} K_{\varsigma}(\alpha_{j,\theta_j,\mathbf{x}} - \alpha) d\mathbf{x}. \quad (9)$$

Typical choices of  $K_{\varsigma}$  are the Gaussian kernel (Parzen) and the Epanechnikov kernel. The choice of  $\varsigma$  is even more

<sup>1</sup>It can be shown that  $p^{\text{MO}}$  exists if and only if  $\frac{M^{(1)2}}{M^{(2)}} < 3/4$ , in which case the solution to (7) is also unique.

crucial and results from a traditional bias-variance trade-off. If the PDF is uniformly bounded and  $C^{s+1}$ , it is well-known that the rate of the quadratic risk of the kernel estimator scales as  $O\left(|\Omega|^{-2s/(2s+1)}\right)$  with the optimal choice  $\varsigma_{\text{opt}} \asymp |\Omega|^{-1/(2s+1)}$ . Typically, for  $s = 2$ , the quadratic risk is  $O(|\Omega|^{-4/5})$  which is much better than the histogram optimal risk  $O(|\Omega|^{-2/3})$ .

**Evolution speed** Suppose the goal is to segment two textures in an image, where we have an exemplar for each. In the language of RBAC, and from (4), this segmentation task boils down to a two region partition problem by minimizing the following functional with respect to the inside and outside regions  $\Omega_{\text{in}}$  and  $\Omega_{\text{out}}$ :

$$G(\Omega_{\text{in}}, \Omega_{\text{out}}) = \sum_{j,\theta_j} \left( |\Omega_{\text{in}}| \underbrace{\int_{\mathcal{X}} \mathcal{D}\left(\text{pdf}_{j,\theta_j}^{\text{in}}(\alpha; \Omega_{\text{in}}), \text{pdf}_{j,\theta_j}^{\text{ref},\text{in}}(\alpha)\right) d\alpha}_{F_{j,\theta_j}(\Omega_{\text{in}})} + |\Omega_{\text{out}}| \underbrace{\int_{\mathcal{X}} \mathcal{D}\left(\text{pdf}_{j,\theta_j}^{\text{out}}(\alpha; \Omega_{\text{out}}), \text{pdf}_{j,\theta_j}^{\text{ref},\text{out}}(\alpha)\right) d\alpha}_{F_{j,\theta_j}(\Omega_{\text{out}})} \right). \quad (10)$$

where  $\text{pdf}_{j,\theta_j}^{\text{in}}$  and  $\text{pdf}_{j,\theta_j}^{\text{out}}$  are the kernel density estimates as given by (9). Using shape derivative tools, as in [1], the following result can be established, see [7] for the proof.

**Theorem 2** *The PDE evolution of the active contour  $\Gamma(\tau)$  corresponding to (10) is:*

$$\frac{\partial \Gamma}{\partial \tau} = \sum_{j,\theta_j} \left( F_{j,\theta_j}(\Omega_{\text{in}}) - F_{j,\theta_j}(\Omega_{\text{out}}) + C_{j,\theta_j}(\Omega_{\text{out}}) - C_{j,\theta_j}(\Omega_{\text{in}}) + \left( (V_{j,\theta_j}(\cdot; \Omega_{\text{in}}) - V_{j,\theta_j}(\cdot; \Omega_{\text{out}})) * K_{\varsigma}(\alpha_{j,\theta_j,\mathbf{x}}) \right) \mathbf{N} \right), \quad (11)$$

where

$$V_{j,\theta_j}(\alpha; \Omega_i) = \partial_1 \mathcal{D}\left(\text{pdf}_{j,\theta_j}^i(\alpha; \Omega_i), \text{pdf}_{j,\theta_j}^{\text{ref},i}(\alpha)\right), \\ C_{j,\theta_j}(\Omega_i) = \int_{\mathcal{X}} V_{j,\theta_j}(\alpha; \Omega_i) \text{pdf}_{j,\theta_j}^i(\alpha; \Omega_i) d\alpha,$$

$\partial_1 \mathcal{D}(\cdot, \cdot)$  is the partial derivative of  $\mathcal{D}(\cdot, \cdot)$  with respect to its first argument, and  $\mathbf{N}$  is the unit normal to the contour.

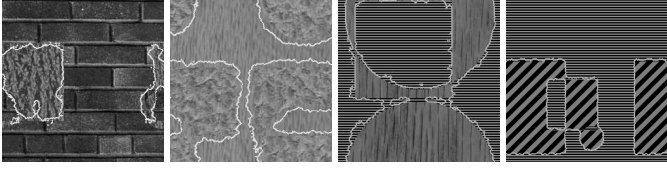
Explicit expressions of  $C_{j,\theta_j}$  and  $V_{j,\theta_j}$  for specific choices of  $\mathcal{D}$  including the KLD and the Hellinger distance are given in [7]. They are omitted here for obvious space limitations.

## 3.2. Unsupervised segmentation and region competition

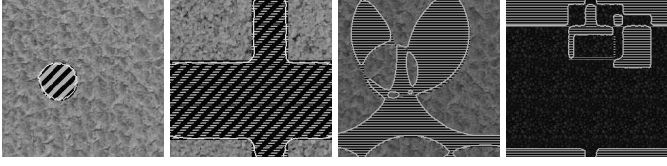
When no exemplar textures are available, it appears natural to make the regions compete. This leads to a maximization problem of the form:

$$G(\Omega_{\text{in}}, \Omega_{\text{out}}) = \sum_{j,\theta_j} \int_{\mathcal{X}} \mathcal{D}\left(\text{pdf}_{j,\theta_j}^{\text{in}}(\alpha; \Omega_{\text{in}}), \text{pdf}_{j,\theta_j}^{\text{out}}(\alpha; \Omega_{\text{out}})\right) d\alpha, \quad (12)$$

where  $\text{pdf}_{j,\theta_j}^{\text{in}}(\alpha; \Omega_{\text{in}})$  and  $\text{pdf}_{j,\theta_j}^{\text{out}}(\alpha; \Omega_{\text{out}})$  are the kernel density estimates as given by (9). In plain words, maximizing this functional will seek the partition in which the coefficients PDFs in the inside and outside regions are the most distinct.



(a) Synthetic images: Supervised (wave-atoms). (b) Synthetic images: Supervised (wavelets).



(c) Synthetic images: Unsupervised (wave-atoms). (d) Synthetic images: Unsupervised (wavelets).



(e) Real images: Unsupervised (wavelets and wave-atoms).

**Fig. 1.** Non parametric texture segmentation examples with different transforms. (a)-(d): synthetic images from the Brodatz database. (e): natural images

With the same notation as in Theorem 2, the evolution speed associated to (12) is given by the following result, see the proof in [7].

**Theorem 3** *The PDE evolution of the active contour  $\Gamma(\tau)$  to maximize (12) is:*

$$\begin{aligned} \frac{\partial \Gamma}{\partial \tau} = & \sum_{j, \theta_j} \left( \frac{1}{|\Omega_{\text{in}}|} \left( - (V_{j, \theta_j}(\cdot; \Omega_{\text{in}}) * K_{\zeta})(\alpha_{j, \theta_j, \mathbf{x}}) + C_{j, \theta_j}(\Omega_{\text{in}}) \right) \right. \\ & \left. + \frac{1}{|\Omega_{\text{out}}|} \left( (V_{j, \theta_j}(\cdot; \Omega_{\text{out}}) * K_{\zeta})(\alpha_{j, \theta_j, \mathbf{x}}) - C_{j, \theta_j}(\Omega_{\text{out}}) \right) \right) \mathbf{N}, \quad (13) \\ V_{j, \theta_j}(\alpha; \Omega_{\text{in}}) = & \partial_1 \mathcal{D} \left( \text{pdf}_{j, \theta_j}^{\text{in}}(\alpha, \Omega_{\text{in}}), \text{pdf}_{j, \theta_j}^{\text{out}}(\alpha, \Omega_{\text{out}}) \right), \\ V_{j, \theta_j}(\alpha; \Omega_{\text{out}}) = & \partial_2 \mathcal{D} \left( \text{pdf}_{j, \theta_j}^{\text{in}}(\alpha, \Omega_{\text{in}}), \text{pdf}_{j, \theta_j}^{\text{out}}(\alpha, \Omega_{\text{out}}) \right), \\ C_{j, \theta_j}(\Omega_{\text{in}}) = & \int_{\mathcal{X}} V_{j, \theta_j}(\alpha; \Omega_{\text{in}}) \text{pdf}_{j, \theta_j}^{\text{in}}(\alpha; \Omega_{\text{in}}) d\alpha, \\ C_{j, \theta_j}(\Omega_{\text{out}}) = & \int_{\mathcal{X}} V_{j, \theta_j}(\alpha; \Omega_{\text{out}}) \text{pdf}_{j, \theta_j}^{\text{out}}(\alpha; \Omega_{\text{out}}) d\alpha. \end{aligned}$$

#### 4. EXPERIMENTAL RESULTS AND DISCUSSION

Fig. 1 displays some examples of non-parametric texture segmentation with two transforms (separable wavelets and wave-atoms) and the supervised and unsupervised approaches. The minimized functional was (1). Beside the speeds provided by Theorem 2 and 3, the active contour evolution speed included

an additional curvature term corresponding to the regularization in (1). In all the experiments,  $\mathcal{D}$  was the KLD and  $K_{\zeta}$  is the Gaussian kernel with a bandwidth chosen according to the above discussion. The synthetic images were generated by randomly combining textures from the Brodatz database. The evolution PDE was implicitly implemented with the level-sets method. Overall, the results are very good. In general, wave-atoms were able to segment more complex textures than separable wavelets owing to their directional selectivity. As expected, wavelets are well adapted whenever the texture is an oscillatory pattern mainly oriented vertically, horizontally or diagonally. With such textures, unsupervised segmentation (texture competition) can be successfully applied to an image with even more than two textures, or one texture and one cartoon part as soon as the oriented texture can be clearly distinguished from the other parts of the image. This is clearly confirmed by the results on real images.

#### 5. REFERENCES

- [1] G. Aubert, M. Barlaud, O. Faugeras, and S. Jehan-Besson. Image segmentation using active contours : Calculus of variations or shape gradients. *SIAM App. Math.*, 63:2128–2154, 2003.
- [2] J.-F. Aujol, G. Aubert, and L. Blanc-Féraud. Wavelet-based level set evolution for classification of textured images. *IEEE Trans. IP*, 12(12):1634–1641, 2003.
- [3] T. Corpetti. An active contour method based on wavelet for texture boundaries. In *ICIP*, pages 1109–1112, 2006.
- [4] M. C. Delfour and J. P. Zolésio. *Shape and geometries*. Advances in Design and Control SIAM, 2001.
- [5] M. N. Do and M. Vetterli. Wavelet-based texture retrieval using generalized gaussian density and kullback-leibler distance. *IEEE Trans. IP*, pages 146–158, 2002.
- [6] S. Jehan-Besson, M. Barlaud, and G. Aubert. Dream2s: Deformable regions driven by an eulerian accurate minimization method for image and video segmentation. *IJCV*, 53(1):45–70, 2003.
- [7] F. Lecellier. *Les contours actifs basés région avec a priori de bruit, de texture et de forme : Application à l'échocardiographie*. PhD thesis, Université de Caen, 2009.
- [8] S. G. Mallat. *A Wavelet tour of signal processing*. Academic Press, 1998.
- [9] F. G. Meyer and R. R. Coifman. Brushlets: a tool for directional image analysis and image compression. *App. Comp. Harm. Anal.*, pages 147–187, 1997.
- [10] G. Peyré. Sparse modeling of textures. *Journal of Mathematical Imaging and Vision*, 34(1):17–31, 2009.
- [11] J. L. Starck, M. Elad, and D. L. Donoho. Redundant multiscale transforms and their application for morphological component analysis. *AIEP*, page 132, 2004.
- [12] M. Unser. Texture classification and segmentation using wavelet frames. *IEEE Trans. IP*, pages 1549–1560, 1995.
- [13] L. Ying and L. Demanet. Wave atoms and sparsity of oscillatory patterns. *App. Comp. Harm. Anal.*, pages 368–387, 2007.